ORIGINAL PAPER

A facile electrochemical synthesis of covellite nanomaterials at room temperature

Yu Jun Yang · Shengshui Hu

Abstract A novel method for the electrochemical synthesis of covellite (CuS) nanoparticles (NPs) in aqueous phase was developed. In this experiment, thioglycerol (TG) is used as the catalyst for the hydrolysis of sodium thiosulfate, the sulfur source for the synthesis of CuS. Cu foil, which acts as the sacrificing anode, is oxidized to Cu^{2+} by applying a potential of 0.5 V while OH^- was produced on the cathode surface at the same time. The production of OH^- facilitates the reaction between Cu^{2+} and thiosulfate under the catalysis of TG. The evolution of hydrogen bubbles effectively prevents the deposition of copper sulfide on the cathode. Copper sulfide sols of "golden-brown", and "dark-green" forms can be obtained by varying the concentration of TG. The "golden-brown" copper sulfide sols are also observed to convert to the green form with time, and the rate of this conversion process is faster at higher temperatures. X-ray diffraction (XRD) and chemical analysis indicate that the "dark-green" form of product is pure hexagonal phase CuS. The obtained CuS NPs were covered by a layer of TG as suggested by Fourier transform infrared (FTIR) data. The size and morphology of the particles are studied by transmission electron microscope (TEM).

Keywords Electrosynthesis · Covellite · Catalysis · Copper sulfide · Nanomaterials

Y. J. Yang · S. Hu (✉)
College of Chemistry & Molecular Sciences, Wuhan University,
Wuhan City, People's Republic of China 430072
e-mail: sshu@whu.edu.cn

Introduction

Recently, electrochemical methods have been widely employed in the synthesis of various nanoparticles (NPs), especially noble metal NPs. Metal NPs such as silver and palladium have been synthesized by electrochemical reduction inside or outside zeolite crystals [1], on 4-amino-benzene monolayer-grafted multiwalled carbon nanotubes [2] and highly oriented pyrolytic graphite electrodes [3]. A sacrificial anode method was developed to prepare metal particles in organic phase [4, 5] and aqueous solution [6, 7]. Metal NPs were also synthesized by the direct electro-reduction of bulk metal ions in aqueous electrolytes with [8–11] and without [12–14] ultrasonic irradiation. Besides the metal NPs, ultrafine magnetite (Fe_3O_4) particles were prepared electrochemically from an iron-based electrode immersed in an alkaline aqueous medium [15]. A novel cyclic voltammetric method was employed to synthesize irregular-shaped PbS NPs [16].

Copper sulfides in different stoichiometries are widely used as *p*-type semiconductors in solar cells, as optical filters, and as superionic materials [17–19]. Due to their unique optical and electrical properties, they are also widely applied in thin films and composite materials [20–25]. Copper sulfide nanocrystals such as nanoparticles, nano-rods, and tubular crystals have been synthesized by solid-state reactions, irradiation, sonochemical, hydrothermal, solvothermal, and chemical vapor deposition (CVD) methods [26–33].

In this study, we report for the first time an electro-chemical method to prepare CuS NPs at ambient conditions. The synthesis of CuS is carried out in water, which is commonly considered as a benign solvent in view of its non-toxicity and abundant natural occurrence. No external excitation system such as ultrasonic and ultraviolet irradi-

ation is required, which significantly simplifies the synthesis procedure. Compared to other synthetic method, this electrochemical method is much easier and more convenient. It will make possible large-scale preparation of the copper sulfides NPs.

Experimental

The copper foil and sodium thiosulfate used in this experiment was purchased from Sinopharm Chemical Reagent. Thioglycerol was obtained from Tokyo Kasei Kogyo. All chemical reagents were of analytical grade and used as received. The electrochemical experiments were performed in a one-compartment cell at room temperature, and were controlled by a potentiostat (model PAR263A, Princeton Advanced Research). A sheet of copper foil (geometric area 0.5×0.5 cm^2), a platinum wire, and SCE (saturated KCl) were employed as the working, counter, and reference electrodes, respectively. The copper foil was treated with diluted nitric acid, cleaned ultrasonically in water and ethanol and then dried with high-purity nitrogen gas before it was used as the working electrode. The distance between counter and working electrodes was kept at 2 cm during the experiment. The aqueous electrolyte solution consisted of $Na_2S_2O_3$ (0.05 M), KNO_3 (0.1 M) and varying concentrations of thioglycerol (TG). A constant potential of 0.5 V/ref was applied to the copper substrate for 1 h in 50-ml as-prepared electrolyte solution under stirring. CuS sol was obtained immediately upon the application of the potential. By adjusting the concentration of thioglycerol (TG) from 0.1 to 0.01 M, the "golden-brown" and "dark-green" colors of CuS colloids were produced. The color transition of copper sulfide was monitored spectrophotometrically with the absorbance recorded between 300 and 900 nm. The produced CuS colloidal solution was centrifuged after mixing with the same volume of ethanol. Then the precipitate was washed with water and absolute ethanol for several times. Black CuS powder was obtained after drying in a vacuum oven at room temperature for 5 h.

Optical absorption spectrum was recorded by using a TU1900 UV–vis spectrophotometer (Beijing Purkinje General Instrument) in the wavelength range of 200~900 nm at room temperature. The X-ray diffraction (XRD) patterns were obtained by Shimadzu XRD-6000 diffractometer with a Ni filter and Cu Kα radiation ($\lambda=1.54056$ Å). Transmission electron microscope (TEM) experiments were carried out employing JOEL 100CX TEM and using an accelerating voltage of 100 kV. The samples used for TEM were prepared by dispersing some products in ethanol followed by ultrasonic vibration for 15 min.

Results and discussion

Copper substrate was used as sacrificial anode in this experiment. The typical cyclic voltammograms of copper electrode in $NaNO_3$ (0.1 M) + $Na_2S_2O_3$ (0.05 M) solution and $NaNO_3$ (0.1 M) + $Na_2S_2O_3$ (0.05 M) + TG (0.01 M) mixed solutions are shown in Fig. 1a. The oxidation peak is at −0.1 V in $NaNO_3$ (0.1 M) + $Na_2S_2O_3$ (0.05 M) (curve 1) while it is at 0.1 V in $NaNO_3$ (0.1 M) + $Na_2S_2O_3$ (0.05 M) + TG (0.01 M) mixed solutions (curve 2). The positive shift of the oxidation peak of Cu is due to the formation of CuS on the copper electrode surface. Without the addition of TG, no CuS can be observed on the copper surface while cycling the potential. Compared to curve 1, reduction peak negatively shifted very significantly (curve 2), which further confirms the formation of CuS on the electrode surface in the presence of TG.

The current–time relationship during the experiment is shown in Fig. 1b. The oxidation current remains almost constant in the first 500 s and then decreased very slowly as the electrolysis continued. The decrease of the oxidation current is not due to the deposition of CuS on copper
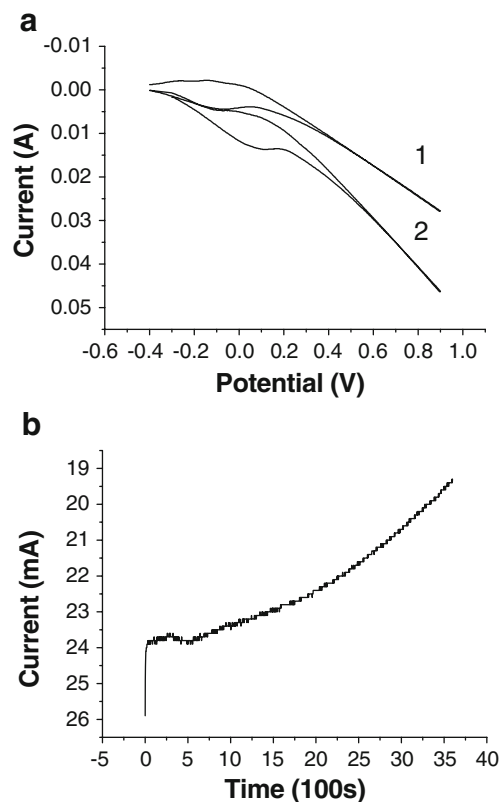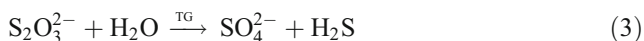

Fig. 1 **a** Cyclic voltammograms for the copper electrode in (curve 1) 0.1 M NaNO3 + 0.05 M $Na_2S_2O_3$; (curve 2) 0.1 M $NaNO_3$ + 0.05 M $Na_2S_2O_3$ + 0.01 M TG mixed solutions without stirring. Scan range: −0.3 to 0.9 V. Scan rate: 100 mV/s. **b** The current–time relationship when applying 0.5 V on the copper electrode in 0.1 M $NaNO_3$ + 0.05 M $Na_2S_2O_3$ + 0.01 M thioglycerol (TG) mixed solutions under stirring

electrode surface, but the decrease of the surface area of copper electrode. This explanation is supported by our observation that no deposition of CuS was observed and the surface area of copper decreased gradually during the reaction. The dissolution of the copper electrode is not uniform; the edges of the electrode dissolved more than other places during the reaction. As the experiment proceeded, the edges of the electrode were gradually etched out, which led to the decrease of the surface area of the electrode and subsequently the oxidation current.

The electrosynthesis of CuS NPs is based on the oxidation of the copper substrate and the reduction of water at a constant potential. The reactions can be written as follows:

$$Cu - 2e \xrightarrow{\text{anode}} Cu^{2+} \tag{1}$$

$$2H_2O + 2e \xrightarrow{\text{cathode}} H_2 \uparrow + 2OH^- \tag{2}$$

$$S_2O_3^{2-} + H_2O \xrightarrow{\text{TG}} SO_4^{2-} + H_2S \tag{3}$$

$$Cu^{2+} + H_2S \rightarrow CuS \downarrow + 2H^+ \tag{4}$$

$$2H^+ + 2OH^- \rightarrow 2H_2O \tag{5}$$

The produced Cu^{2+} reacts with thiosulfate to form CuS under the catalysis of TG while TG also protects the produced CuS NPs from aggregation. The addition of TG is crucial for the synthesis of CuS. This is supported by the observation that without the addition of TG, no CuS can be produced. With the catalysis of TG, it can be observed that the electrolyte around the cathode changed in color from colorless to yellow immediately upon the application of potential. The appearance of the yellow color reveals the formation of CuS NPs. With 0.01 M TG, highly stable "dark-green" CuS colloid solution was produced. No CuS precipitate can be observed at the bottom of the beaker. However, when the concentration of TG was decreased to 10^{-3} M, a large amount of CuS precipitate was observed. Thus, we conclude that TG is not only the catalyst for the synthesis of CuS, but also acts as the capping agent of the produced CuS NPs.

It is well-known that a $S_2SO_3^{2-}$ ion can hydrolyze to release a S^{2-} anion [34, 35], which reacts with Cu^{2+} to produce copper sulfide (CuS or $Cu_{2-x}S$). However, in a system containing only copper sulfate, sodium thiosulfate, and water the hydrolysis of thiosulfate is a very slow process at ambient conditions. It takes 1 week to produce black-green $Cu_{2-x}S$ in the mixed solution of $CuSO_4$ and $Na_2S_2O_3$ at room temperature and ambient pressure [34].

The catalytic effect of thioglycerol on the hydrolysis of thiosulfate has been thoroughly studied in our previous report [35]. It was found out that with the catalysis of thioglycerol (TG), Cu^{2+} can react easily with thiosulfate under ambient conditions.

Our recent study indicated that, under the catalysis of TG, the rate of the hydrolysis of thiosulfate increased as the solution pH increased. In an aqueous solution containing $Na_2S_2O_3$ (0. 005 M), $CuSO_4$ (0.001 M), and TG (0.005 M), the pH of which is 7.2, it took 1 h for the solution to change from transparent and colorless to black [35]. When the solution pH was adjusted to 8.0 by adding concentrated NaOH solution, the reaction rate was significantly increased. At pH 8.0, the solution changed from colorless to black in just 20 min. This discovery gave the above proposed mechanism (Eqs. 3 and 4) a strong support. As shown in Eq. 5, the presence of OH⁻ could consume the produced H⁺ and facilitate the production of CuS. However, at high solution pH, the formation of $Cu(OH)_2$ precipitate is inevitable. At pH 10.0, a significant amount of $Cu(OH)_2$ precipitate was observed at the bottom of the flask.

To obtain a high reaction rate between Cu^{2+} and thiosulfate, we should carry out the reaction in an alkaline environment while avoiding the formation of $Cu(OH)_2$ precipitate at the same time. An electrochemical method was proposed to achieve this purpose. Cu^{2+} and OH⁻ were produced on the anode and cathode surface, respectively, after a constant potential (0.5 V) was applied. Cu^{2+} migrated from electrode surfaces under stirring and reacted with thiosulfate under the catalysis of TG. The farther from the cathode surface, the lower the solution pH is. Keeping the distance between cathode and anode constant at 2 cm, the solution pH in the vicinity of cathode and anode was measured with a pH meter under typical experimental condition.

In the vicinity of the cathode and anode surface, the solution pH values were about 13.1 and 10.3, respectively. Decreasing the stirring rate, it was found out that the pH difference increased immediately. This phenomenon supported our supposition that significant solution pH difference between the cathode and anode was maintained even under magnetic stirring. It was observed that the solution around the cathode surface changed in color from colorless to yellow immediately upon the application of potential. This phenomenon further confirmed our supposition that higher solution pH favors the reaction. The farther from the anode, the lower the concentration of Cu^{2+} is.

The concentration of Cu^{2+} around the cathode surface is pretty low due to the slow release of Cu^{2+} from the copper sacrificial anode and the quick reaction rate between Cu^{2+} and thiosulfate around the cathode. Therefore, no formation of $Cu(OH)_2$ precipitate was observed during the reaction,
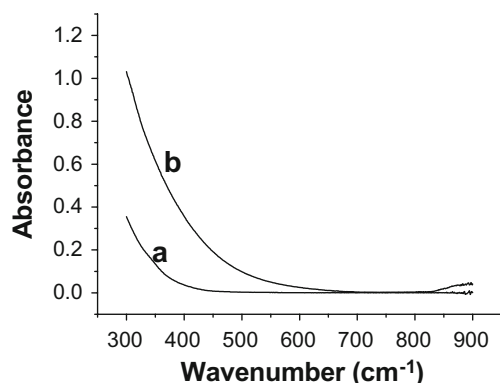
Fig. 2 UV–vis spectrum of as-prepared CuS produced by applying the potential of 0.5 V in **a** 0.1 M NaNO$_3$ + 0.05 M Na$_2$S$_2$O$_3$+ 0.1 M thioglycerol (TG); (**b**) 0.1 M NaNO$_3$ + 0.05 M Na$_2$S$_2$O$_3$+ 0.01 M TG mixed solutions for 1 h

although the solution pH is very high around the cathode. The final product is highly stable copper sulfide colloid solution. Although the reaction rate between Cu^{2+} and thiosulfate is very quick around the cathode, there is no deposition of copper sulfide on the cathode surface. This is because a large amount of bubbles evolved at the cathode surface when the potential was applied.

The formation of hydrogen on the cathode helps to remove the copper sulfide from the electrode surface. During this experiment, a competition between two different cathode surface processes exists. One process is the copper sulfide particles formation in the vicinity of cathode surface, where solution pH is much higher than the bulk solution, and the other is the copper sulfide deposition on cathode. The evolution of hydrogen gas greatly enhances the former and effectively reduces the latter.

The reaction rate between Cu^{2+} and thiosulfate around anode is very slow because the solution pH around the anode is much lower than that around the cathode. Thus, the deposition of CuS on the anode surface is not a serious
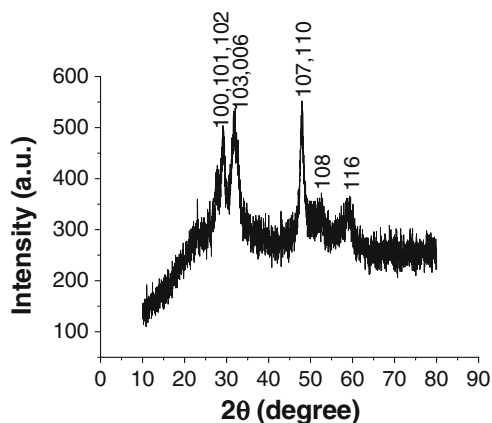
problem. The application of stirring could greatly enhance the diffusion of the produced CuS NPs from the anoxic vicinity to the bulk solution and effectively prevented the deposition of CuS on the electrode surface. Experimental results showed that no deposition of CuS can be observed on the copper surface even under very mild magnetic stirring.

By adjusting the concentration of TG, copper sulfide colloid solutions with different colors were obtained. The UV–vis spectra of the as-prepared samples were recorded in the range of 300–900 nm. In Fig. 2 is shown the representative UV–vis spectra of golden-brown copper sulfide colloid solution prepared in NaNO$_3$ (0.1 M) + Na$_2$S$_2$O$_3$ (0.05 M) + TG (0.1 M) (Fig. 2a) and dark-green copper sulfide colloid solution prepared in NaNO$_3$ (0.1 M) + Na$_2$S$_2$O$_3$ (0.05 M) + TG (0.1 M) (Fig. 2b). Both samples absorbed in the spectral region between 250 and 650 nm. However, only for the "dark-green" form of copper sulfide, an increased absorption band extending into the near-IR region can be observed, which is characteristic of covellite (CuS) [36].

It was also found out that the "golden-brown" form of copper sulfide colloid solution may convert to the dark-green form of copper sulfide. The rate of the conversion increased with the increase of the temperature. At room temperature, it takes 72 h for the "golden-brown" form of copper sulfide colloid solution to convert into the "dark-green" form. Increasing the temperature to 80 °C, it only takes about 45 min for the "golden-brown" form to convert into the "dark-green" form. This is in good agreement with the discovery of J. S. Wen et. al [36]. According to their research, the "golden-brown" sol is a poorly crystalline form of covellite, and this poorly crystalline covellite recrystallizes to crystalline covellite (the "dark-green" form) at a rate that depends on the temperature and oxygen concentration of the sol. Investigation on the photolumi-nescence of the "dark-green" form of CuS revealed no
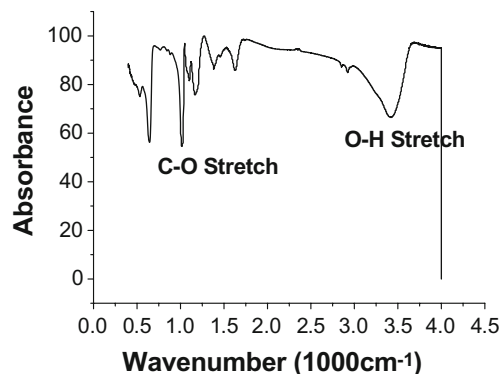

Fig. 3 XRD patterns of hexagonal phase CuS obtained after the "golden-brown" CuS sol produced in 0.1 M NaNO$_3$ + 0.05 M Na$_2$S$_2$O$_3$+ 0.1 M thioglycerol (TG) mixed solutions converted into "dark-green" form

Fig. 4 Fourier transform infrared spectra of TG protected CuS produced by applying the potential of 0.5 V in 0.1 M NaNO$_3$ + 0.05 M Na$_2$S$_2$O$_3$+ 0.01 M thioglycerol (TG) mixed solutions for 1 h

Fig. 5 TEM images of CuS NPs obtained after the "golden-brown" CuS sol produced in 0.1 M NaNO$_3$ + 0.05 M Na$_2$S$_2$O$_3$+ 0.1 M thioglycerol (TG) mixed solutions converted into "dark-green" form
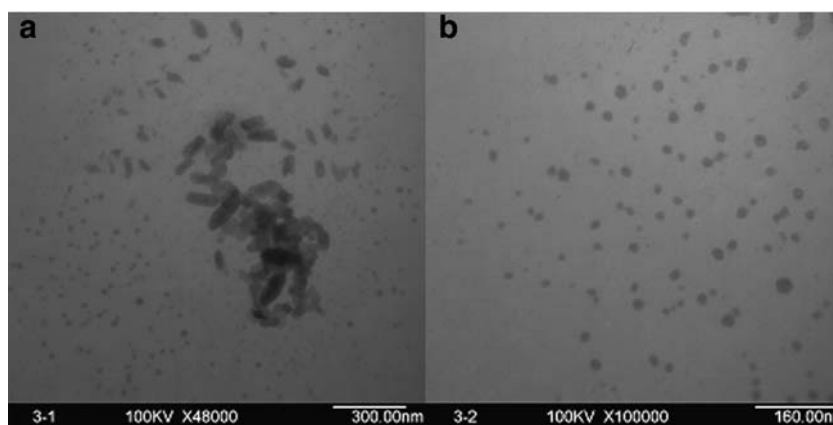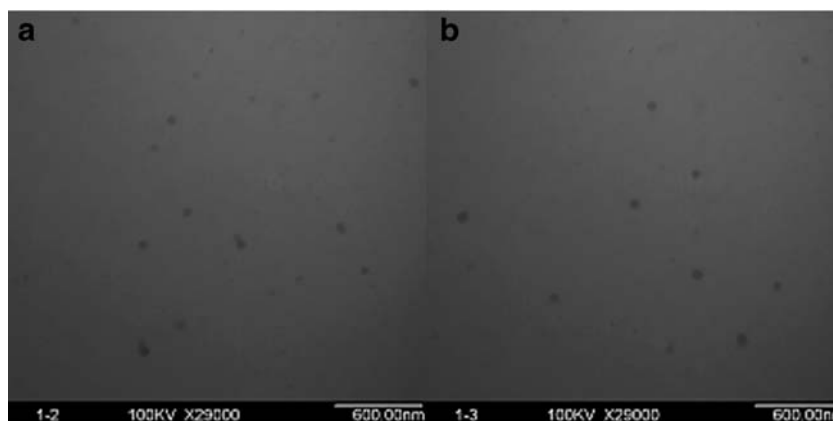

emission in the range 400~800 nm, which is ascribed to the formation of covellite [37–39].

X-ray diffraction is carried out to study the structure of the CuS NPs. Figure 3 presents the XRD patterns of the CuS precipitate (obtained from the "dark-green" form of CuS). The broadness of the diffraction peaks indicated the nanocrystalline nature of the product. All the reflections can be indexed to the hexagonal crystal CuS according to the literature pattern for CuS (JCPDS File No. 36-379). The XRD analysis further confirmed that no Cu(OH)$_2$ was produced in the reaction.

The Fourier transform infrared (FTIR) spectrum of the produced rod-shaped CuS crystals in Fig. 4 shows a strong and broad O–H stretching band at 3,500 cm^{-1} and a strong C–O stretching band at 1,100 cm^{-1}. The FTIR spectra confirm that the CuS crystals are capped with TG, and the TG molecule is not leached out during several washings of the CuS crystals. Chen SW et. al. have observed that differential pulse voltammetry (DPV) of purified monolayer protected gold clusters exhibit quantized double-layer (QDL) capacitance charging [40, 41]. However, in this experiment, quantized double-layer (QDL) charging peaks cannot be observed in the DPV of the purified TG-protected CuS NPs obtained from the synthesis reaction mixture.

The size of the copper sulfide NPs of the "golden-brown" form produced in NaNO$_3$ (0.1 M) + Na$_2$S$_2$O$_3$ (0.05 M) + TG (0.1 M) is about 80–120 Å. For the "golden-brown" form, it is extremely difficult to precipitate the CuS NPs by centrifuging for 30 min at 12,000 rpm. However, after it converted into "dark-green" form at room temperature, the CuS NPs can be easily precipitated. The TEM images of the obtained CuS NPs are shown in Fig. 5, which clearly show that the particles are the mixture of spherical NPs and nanorods (Fig. 5a). Both the spherical NPs (Fig. 5b) and nanorods are 30 nm in diameter, while the length of the nanorods is about 100 nm.

The "dark-green" form of CuS sols was prepared directly in NaNO$_3$ (0.1 M) + Na$_2$S$_2$O$_3$ (0.05 M) + TG (0.01 M) mixed solutions. The TEM images verify further that the products are spherical NPs with 50 nm in diameter (Fig. 6).

Conclusions

In summary, a novel potentiostatic method was successfully developed for the synthesis of CuS NPs. With copper as sacrificial anode, copper sulfide sols were synthesized by applying a constant potential of 0.5 V in a sodium

Fig. 6 TEM images of CuS NPs produced by applying the potential of 0.5 V in 0.1 M NaNO$_3$ + 0.05 M Na$_2$S$_2$O$_3$+ 0.01 M thioglycerol (TG) mixed solutions for 1 h

thiosulfate and thioglycerol aqueous solution. The results showed that the production of OH$^-$ at the cathode facilitates the reaction between Cu^{2+} and S$_2$SO$_3^{2-}$, while the evolution of hydrogen effectively prevents the deposition of copper sulfide on the cathode surface. In this experiment, TG not only acts as the catalyst for the hydrolysis of thiosulfate but also the stabilizer of the produced NPs. "Golden-brown" CuS sol was produced at higher TG concentration, while the "dark-green" form of CuS was produced at lower TG concentration. The "golden-brown" CuS sol is a poorly crystalline form of covellite, which converts to crystalline covellite (the "dark-green" form) at a rate that depends on the temperature of the sol.

References

1. Zhang YH, Chen F, Zhuang JH, Tang Y, Wang DJ, Wang YJ, Dong AG, Ren N (2002) Chem Commun 23:2814
2. Guo DJ, Li HL (2004) Electrochem Commun 6:999
3. Mazur M (2004) Electrochem Commun 6:400
4. Reetz MT, Helbig W (1994) J Am Chem Soc 116:7401
5. Rodrigues-Sanchez L, Blanco MC, Lopez-Quintela MA (2000) J Phys Chem B 104:9683
6. Yu YY, Chang SS, Lee CL, Wang CRC (1997) J Phys Chem B 101:6661
7. Mohamed MB, Ismail KZ, Link S, El-Sayed MA (1998) J Phys Chem B 102:9370
8. Liu YC, Li HL (2004) Electrochem Commun 6:1163
9. Reisse J, Francois H, Vandercammen J, Fabre O, Mesmaeker AKD, Maerschalk C, Delplancke JL (1994) Electrochim. Acta 39:37
10. Delplancke JL, Dille J, Reisse J, Long GJ, Mohan A, Grandjean F (2000) Chem Mater 12:946
11. Shen LM, Yao JL, Gu RA (2007) Acta Chimica Sinica 65:203
12. Ma HY, Yin BS, Wang SY, Jiao YL, Pan W, Huang SX, Chen SH, Meng FJ (2004) Chem Phys Chem 5:68
13. Yin BS, Ma HY, Wang SY, Chen SH (2003) J Phys Chem B 107:8898
14. Huang CJ, Chiu PH, Wang YH, Chen KL, Linn JJ, Yang CF (2006) J Electrochem Soc 153:D193
15. Franger S, Berthet P, Berthon J (2004) J Solid State Eletrochem 8:218
16. Yang YJ, He LY, Zhang QF (2005) Electrochem Comm 7:361
17. Grozdanov I, Najdoski M (1995) J Solid State Chem 14:469
18. Nascu C, Pop I, Ionescu V, Indrea E, Bratu I (1997) Mater Lett 32:73
19. Hermann AM, Fabick L (1983) J Cryst Growth 61:658
20. Wang M, Sun L, Fu X, Liao C, Yan C (2000) Solid State Commun 115:493
21. Hu J, Deng B, Zhang W, Tang K, Qian Y (2001) Int J Inorg Mater 3:639
22. Takase K, Koyano M, Shimizu T, Makihara K, Takahashi Y, Takano Y, Sekizawa K (2002) Solid State Commun 123:531
23. Qiao Z, Xie Y, Xu J, Zhu Y, Qian Y (1999) J Colloid Interface Sci 214:459
24. Zhang Y, Qiao Z, Chen X (2002) J Solid State Chem 167:249
25. Wang H, Zhang J, Zhao X, Xu S, Zhu J (2002) Mater Lett 55:253
26. Lu J, Zhao Y, Chen N, Xie Y (2003) Chem Lett 32:30
27. Wang C, Tang K, Yang Q, Bin H, Shen G, Qian Y (2001) Chem Lett 494
28. Zhang P, Gao L (2003) J Mater Chem 13:2007
29. Wu CY, Yu SH, Chen SF, Liu GN, Liu BH (2006) J Mater Chem 16:3326
30. Qin AM, Fang YP, Ou HD, Liu HQ, Su CY (2005) Cryst Growth Design 5:855
31. Zhang HT, Wu G, Chen XH (2006) Mater Chem Phys 98:298
32. Ji HM, Cao JM, Feng J, Chang X, Ma XJ, Liu JS, Zheng MB (2005) Mater Lett 59:3169
33. Tan CH, Zhu YL, Lu R, Xue PC, Bao CY, Liu XL, Fei ZP, Zhao YY (2005) Mater Chem Phys 91:44
34. Ni YH, Wang F, Liu HJ, Liang YY, Yin G, Hong JM, Ma X, Xu Z (2003) Inorg Chem Comm 6:1406
35. Yang YJ, Xiang JW (2005) Appl Phys A 81:1351
36. Ewen JS, Franz G, Brett AS, Thomas WH (1991) Langmuir 7:2917
37. Zhang P, Gao L (2003) J Mater Chem 13:2007
38. Dixit SG, Mahadeshwar AR, Haram SK (1998) Coll Surf A 133:69
39. Haram SK, Mahadeshwar AR, Dixit SG (1996) J Phys Chem 100:5868
40. Chen SW, Templeton AC, Murray RW (2000) Langmuir 16:3543
41. Chen SW, Murray RW. J Phys Chem B 103:9996